Journal of Maps

ISSN: (Print) (Online) Journal homepage: https://www.tandfonline.com/loi/tjom20

Geomorphology of the Anversa degli Abruzzi badlands area (Central Apennines, Italy)

Jacopo D'Intino , Marcello Buccolini , Elena Di Nardo , Gianluca Esposito & Enrico Miccadei

To cite this article: Jacopo D'Intino , Marcello Buccolini , Elena Di Nardo , Gianluca Esposito & Enrico Miccadei (2020) Geomorphology of the Anversa degli Abruzzi badlands area (Central Apennines, Italy), Journal of Maps, 16:2, 488-499, DOI: 10.1080/17445647.2020.1780169

To link to this article: https://doi.org/10.1080/17445647.2020.1780169

JOURNAL OF MAPS
2020, VOL. 16, NO. 2, 488–499
https://doi.org/10.1080/17445647.2020.1780169

Taylor & Francis
Taylor & Francis Group

Science

Geomorphology of the Anversa degli Abruzzi badlands area (Central Apennines, Italy)

Jacopo D'Intino [a], Marcello Buccolini [a], Elena Di Nardo[a], Gianluca Esposito [a] and Enrico Miccadei [a,b]

[a]Department of Engineering and Geology, Laboratory of Tectonic Geomorphology and GIS, Università degli Studi 'G. d'Annunzio' Chieti-Pescara Chieti Scalo (CH), Italy; [b]Istituto Nazionale di Geofisica e Vulcanologia (INGV) Roma, Italy

ABSTRACT

This work presents the geomorphology of the Anversa degli Abruzzi badlands (also called *calanchi*, a typical italian landform) area, located in the Abruzzo Region (Central Apennines, Italy). The map is the result of morphometric and geomorphological analyses, performed at the badland scale, and incorporates three main sections including orography and hydrography, main geomorphological map, and multi-temporal photogeological analysis. The aim of this work is to provide the basis for the recognition of geomorphological features linked to the fluvial environment. Specifically, the study is focused on the Anversa degli Abruzzi *calanchi* system and it contributes to improving the understanding of this landscape evaluating the geomorphological processes that control its morphometric features and its spatial and temporal evolution.

ARTICLE HISTORY
Received 2 March 2020
Revised 24 May 2020
Accepted 5 June 2020

KEYWORDS
Geomorphology; photogeology; badlands; gully erosion; Central Italy

1. Introduction

An extensive geomorphological analysis of the Adriatic hilly-piedmont area of the Central Apennines allowed researches focused on the geomorphological evolution, morphotectonic implications, and climatic characterization of badland systems, since the first half of the 1900s (Alexander, 1980; Castiglioni, 1933; Ciccacci et al., 2008; Coltorti et al., 1979; Demangeot, 1965; Farabollini et al., 1992; Magny et al., 2002; Moretti & Rodolfi, 2000; Nisio et al., 1996; Rodolfi & Frascati, 1979; Vittorini, 1971); more recent studies concentrate on morphometric analysis highlighting similarities between badlands and fluvial systems (Buccolini & Coco, 2010; Buccolini & Coco, 2013; Buccolini et al., 2012; Caraballo-Arias et al., 2015; Caraballo-Arias & Ferro, 2017; Di Stefano & Ferro, 2019; Neugirg et al., 2016; Vergari et al., 2019).

In this study, we present a 1:2500 scale geomorphological map of the Anversa degli Abruzzi badlands area, located in the Central Abruzzo area (Marsica region; Figure 1). It has been implemented within a GIS environment by means of morphometric analysis of orography and hydrography; detailed geological and geomorphological field mapping, and finally of geomorphological evolution via a multi-temporal photogeological analysis.

The main map incorporates three principal sections:

(i) orography and hydrography;
(ii) main geomorphological map (scale 1:2500);
(iii) multi-temporal evolution scheme.

This study provides a basis for the recognition of geomorphological processes that control the morphometry of a badlands system and it represent a significant tool to improve knowledge about this typical Italian landscape. It allows us to define the main phases of *calanchi* evolution, resulting from slope-gravity processes, water runoff.

2. Study area

The Anversa degli Abruzzi badlands area (whose toponym is *il Caccavone*) is located in the Central Apennines, an arc-shaped and asymmetric mountain range which is the result of the Neogene-Quaternary evolution of a chain-foreland-foredeep system generated through the westward subduction of the Adriatic microplate (Carminati & Doglioni, 2012; Miccadei et al., 1998; Miccadei et al., 2017; Miccadei et al., 2018; Piacentini et al., 2015). The chain is made up of thrust sheets resulting from the deformation of Meso-Cenozoic paleogeographic domains (carbonate platforms and margins, slope and basin) consisting of pre-orogenic thick limestone and marl-limestone sequences (Miccadei et al., 2019 and references therein).

Orogenic compressional tectonics along NW–SE to N–S-oriented thrusts affected the Central Apennines causing the complex superimposition of the tectonic units one over the other and over syn-orogenic pelitic-arenaceous turbiditic sequences.

CONTACT Enrico Miccadei enrico.miccadei@unich.it Department of Engineering and Geology, Laboratory of Tectonic Geomorphology and GIS, Università degli Studi 'G. d'Annunzio' Chieti-Pescara, Via dei Vestini 31, 66100 Chieti Scalo (CH), Italy; Istituto Nazionale di Geofisica e Vulcanologia (INGV), Sezione Roma 1, Via di Vigna Murata 605, 00143 Roma, Italy

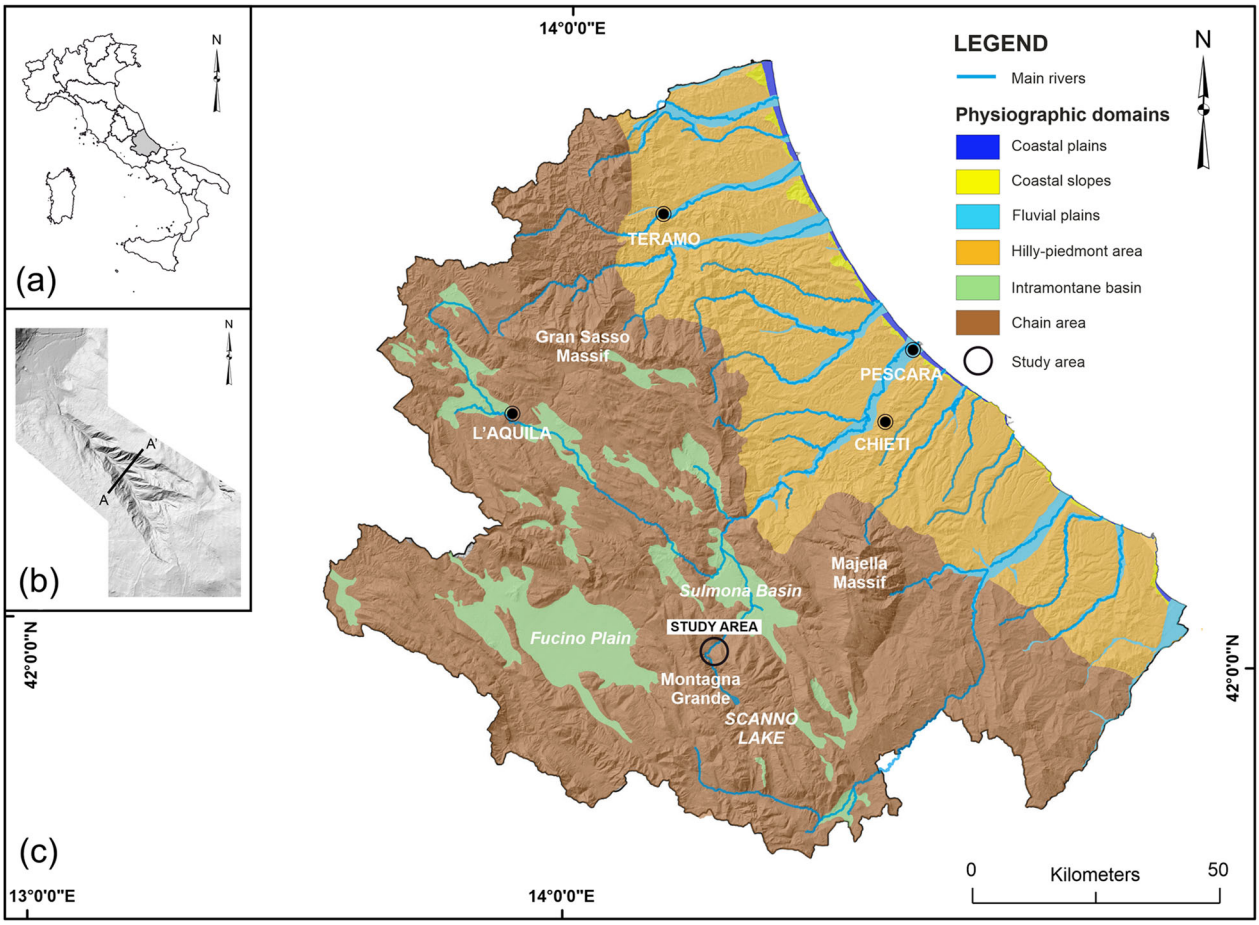

Figure 1. Location map of: (a) Abruzzo in Italy; (b) location of the schematic geomorphological profile inside the study area (see Figure 7); (c) Study area (black circle) in the physiographic setting of the Abruzzo Region.

The compressional tectonics was followed by strike-slip tectonics along mostly NW–SE to NNW–SSE-oriented faults, largely masked by younger extensional tectonics, contributing to define a more complex tectonic setting. Since the Lower Pleistocene, the orogen underwent regional uplifting (Carminati & Doglioni, 2012; Miccadei et al., 2017). Post-orogenic tectonics is characterized by extensional kinematics which affects the chain still today, as highlighted by recent major earthquakes (up to M7.0; Fucino, January, 1915; L'Aquila, April, 2009; Central Italy, August–till today, 2016–2017; Rovida et al., 2019; ISIDe Working Group, 2016), with NW–SE-oriented extensional fault systems and which caused the formation of intermontane basins, such as Fucino Plain and Sulmona Basin (Ascione et al., 2008; Capelli et al., 1997; Ciccacci et al., 1999; Corrado et al., 1996; Ghisetti & Vezzani, 1993; Mattei & Miccadei, 2001; Miccadei, 1993; Miccadei et al., 2014; Miccadei et al., 2018; Piacentini & Miccadei, 2014; Vezzani et al., 2010).

The geomorphological evolution began with the emersion of the orogen at least from Miocene (in the chain area) and it is closely connected with a complex combination of endogenous (morphotectonics) and exogenous processes (slope, fluvial, karst and glacial processes). The combination of these factors with Quaternary climate fluctuations led to the succeeding of some morphogenetic phases, resulting in the reorganization of the landscape to the present-day setting (Miccadei et al., 2017 and references therein).

The study area (Figure 2) is located in the chain area of the Abruzzo Region and is set in the Sagittario River basin which incorporates a 48-km-long main river. It is called Tasso Stream, in the southern stretch, and flows with an S-N direction into the Scanno Lake, from where it flows through and incises the Sagittario gorges in a SE-NW direction. Near Anversa degli Abruzzi village, it describes a 90° sharp bend to NE and flows towards Sulmona Basin making a wide incision transversal to the main ridges of the area (Montagna Grande, Mt. Genzana) (Miccadei et al., 2019).

From a geological standpoint, the area is made up of three main paleogeographic domains: (i) the Mesozoic-Cenozoic Lazio-Abruzzi carbonate platform with its proximal slope, (ii) the Cenozoic carbonate ramp, and (iii) the turbiditic succession referred to the Messinian evaporitic foredeep (Carabella et al., 2019; Miccadei et al., 2017). The oldest units (Upper Triassic-Lower Jurassic) outcrops on the La Difesa ridge, while the proximal slope unit (Upper Jurassic-Paleogene) and the carbonate ramp domain (Eocene-Messinian pre-evaporitic) are spread between Anversa

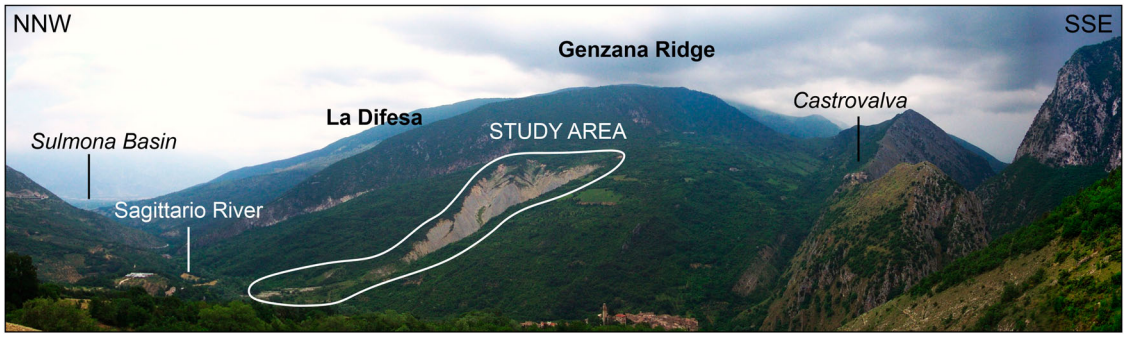

Figure 2. Panoramic view of the Anversa degli Abruzzi badlands area.

degli Abruzzi and Castrovalva towns on the west side of the study area. These units consist of dolomitic limestones and limestones sequences and constitute the pre-orogenic succession. The syn-orogenic succession consists of an evaporitic siliciclastic unit and it represents the substratum of the badlands area. Post-orogenic continental deposits are related to various morphogenetic environments, such as slope (slope and landslide deposits) and fluvial dynamics (Beneo, 1938; Calista et al., 2016; Cassetti, 1900; Corrado et al., 1996; Miccadei et al., 2014; Miccadei et al., 2019). From a climatic point of view, the study area is characterized by a Mediterranean climate with cold winters and heavy snowfalls, dry summers with some afternoon rainfalls and dry springs (Di Lena et al., 2012).

3. Methods

The badlands area was investigated using an integrated approach that incorporates: (i) morphometric analysis of orography and hydrography, (ii) geological and geomorphological field mapping and (iii) the multi-temporal photogeological analysis (see Table 1).

The morphometric analysis of orography and hydrography was carried out with the GIS software (ArcGis, version 10.6.1). Vector topographic data were extracted from 1 m LiDAR data provided by Ministero dell'Ambiente e della Tutela del Territorio e del Mare (http://www.minambiente.it). The analysis was focused on the investigation of the main orographic features, such as slope analysis and aspect analysis (Strahler, 1957), and on the detailed definition of the badland drainage system through the calculation of morphometric parameters such as badlands area (A_{2D}); length (L); perimeter (P); L/P (a ratio of the stream pattern geometry) and basin slope (S); drainage frequency (F) and density (D), Melton ratio (F/D^2; Melton, 1957); hierarchical order which is a numerical measure of the branching of a stream (O; Strahler, 1957); bifurcation ratio, which is a ratio of the number of stream branches of a given order to the number of stream branches of the next higher order; (R_b; Horton, 1945), and circularity ratio, which is the ratio of basin area to the area of circle having the same perimeter as the basin (R_C; Miller, 1953).

A detailed geological and geomorphological field survey was carried out on a 1:2000 scale topography to map lithologies (bedrock and quaternary continental deposits) and the geomorphological features. It was performed according to the guidelines of the Geological Survey of Italy (SGN, 1994), and was also in accordance with the literature concerning geological and geomorphological mapping (D'Orefice & Graciotti, 2014; Miccadei et al., 2012; Miccadei et al., 2019;

Table 1. Workflow scheme of the creation of the geomorphological map of the Anversa degli Abruzzi badlands area.

Activities	Data	Elaboration and GIS analysis	Results
Morphometry of orography and hydrography	**LiDAR** 1 m **Vector topography** Scale 1:2000	**Analysis of orographic and hydrographic parameters**	**Slope map** **Aspect map** **Density map** **Hierarchic order map**
Geology and geomorphological field mapping	**Geological field mapping** Scale 1:2000 **Geomorphological field mapping** Scale 1:2000	**Field mapping of bedrock and superficial deposits** **Landforms mapping and analysis**	**Geomorphological map** Scale 1:2500
Multi-temporal photogeological analysis	**Aerial photos** Scale 1:33,000 **Orthophotos** Scale 1:10,000 Scale 1:5000 **Satellite images** Scale 1:1000	**Aerial photo interpretation and photogeological analysis**	**Multi-temporal maps** Alluvial fan area Badlands area Active area

Table 2. Morphometric parameters of the badland area. O, Rb, RC and F/D^2 are dimensionless factors.

Morphometric parameters	Unit of measure	Value
Basin area (A_{2D})	(m^2)	512,602
Badland area (A_C)	(m^2)	354,678
Perimeter (*P*)	(m)	4496
Length (L)	(m)	1631
Slope (S)	(°)	21
Length/Slope (L/S)	(m/°)	77.6
Frequency (F)	(m^{-2})	0.000247
Density (D)	(m^{-1})	0.0185
Strahler's order (O)		5th
Bifurcation ratio (R_b)		2–4
Circularity ratio (R_C)		0.31
Melton ratio (F/D^2)		0.719

Salvador, 1994). In order to highlight the main geomorphological features of the *calanchi* area, a geomorphological profile was also realized. Finally, geomorphological investigations were supported by photogeological analysis performed using stereoscopy from aerial photo and GIS analysis for orthophotos (Table 1). This analysis allowed to get semi-quantitative data about alluvial fan, active flooding sector, flooding channel, eroded area, and hydrographic pattern type, according to Twidale, 2004 and references therein.

4. Results

4.1. Orography and hydrography

The study area is characterized by an NW–SE-oriented slope with an elevation ranging from ~465 m a.s.l., in the NW sector (at the confluence with the Sagittario River), to ~1050 m a.s.l. in the northernmost sector of the study area. The average slope of the badland system is ~20°, with the highest values >60° in the southern sector. The principal aspect of the eastern slope is W, NW, and subordinately S, while in the western slope is N-NE. The *calanchi* area (A_c) reaches 287,917 m^2. The longitudinal profile shows a concave to convex shape and an evident step at the upper badland limit; the transversal profile has a clear V-shape with steep slopes.

The main hydrographic parameters calculated for the study area summarized in Table 2. The hydrography is characterized by several minor and ephemeral stream channels (Figure 3). The drainage network shows a mainly dendritic, locally sub-dendritic subparallel drainage pattern; highlighted by L/P ratio (77.6 m/°). D values are higher in the intermediate sector of the incision, and the Melton ratio (F/D^2) provides a constant equal to 0.719. The stream is highly hierarchized and reaches the 5th order; the 1st order streams are present at the top of the badland area, while the 5th order is located at the bottom. The bifurcation ratio ranges from 2 to 4; the minimum value is between the 4th and the 5th order while the maximum one is between the 2nd and the 3rd order. Between 1st and 2nd the bifurcation ratio is 3.14 while for 3rd and 4th is 3.5. The Circularity ratio is 0.31, highlighting a stretched shape.

4.2. Lithology

Outcropping lithologies were classified in marine and continental deposits. The marine deposits are characterized by clayey-pelitic rocks with gypsum layers, referred to the Messinian evaporitic syn-orogenic turbiditic deposits (Corrado et al., 1996; ISPRA, 2014; Miccadei et al., 2014; Miccadei et al., 2019;); subordinately, calcareous-dolomitic bedrock outcrops on the La Difesa ridge. Post-orogenic continental deposits are widespread in the area and they can be referred to fluvial and slope environments. They are listed in the following paragraphs, from the oldest to the youngest (numbers refer to the main map and its relative legend) and they were referred to the units of the CARG 378 sheet (ISPRA, 2014).

4.2.1. Pre-orogenic marine deposits

4.2.1.1. Dolomitic limestones (8). They are composed of massive grayish dolomitic limestones locally well stratified with pluri-decimetric strata, outcropping on La Difesa ridge because of a tectonic contact with the Clays unit (7). This unit is dated to the Upper Triassic-Lower Jurassic (Sinemurian) interval (Miccadei et al., 2014).

4.2.2. Syn-orogenic marine deposits

4.2.2.1. Clays (7). It is made up of poorly stratified clay and well-stratified leaden silty clays (Figure 4(a)); locally cross laminations are present. From decimetric to plurimetric gypsum elements (the most evident are indicated by a black ring in the main map) are present, often inside a Havana arenitic chalk, made of millimetric and centimetric crystals; very thin white gypsum levels are present. This unit is in tectonic contact with unit 8 (see also the geological scheme of the Sagittarius Valley in the main map). Clays are dated to Messinian evaporitic (Corrido et al., 1996; Maccabee et al., 2014).

4.2.3. Post-orogenic continental deposits

4.2.3.1. Ancient slope deposits (6). They are composed of centimetric and decametric stratified clasts, both cemented and loose. These outcrop at the top of the badlands incision (Figure 4(b)) on the clayey substrate by an erosive limit. They refer to to as the Upper Pleistocene (Miccadei et al., 2014).

4.2.3.2. Slope deposits (5). This unit is made up of heterometric loose clasts with moderate matrix and outcrop on slope breaks. They refer to the Holocene (Miccadei et al., 2014).

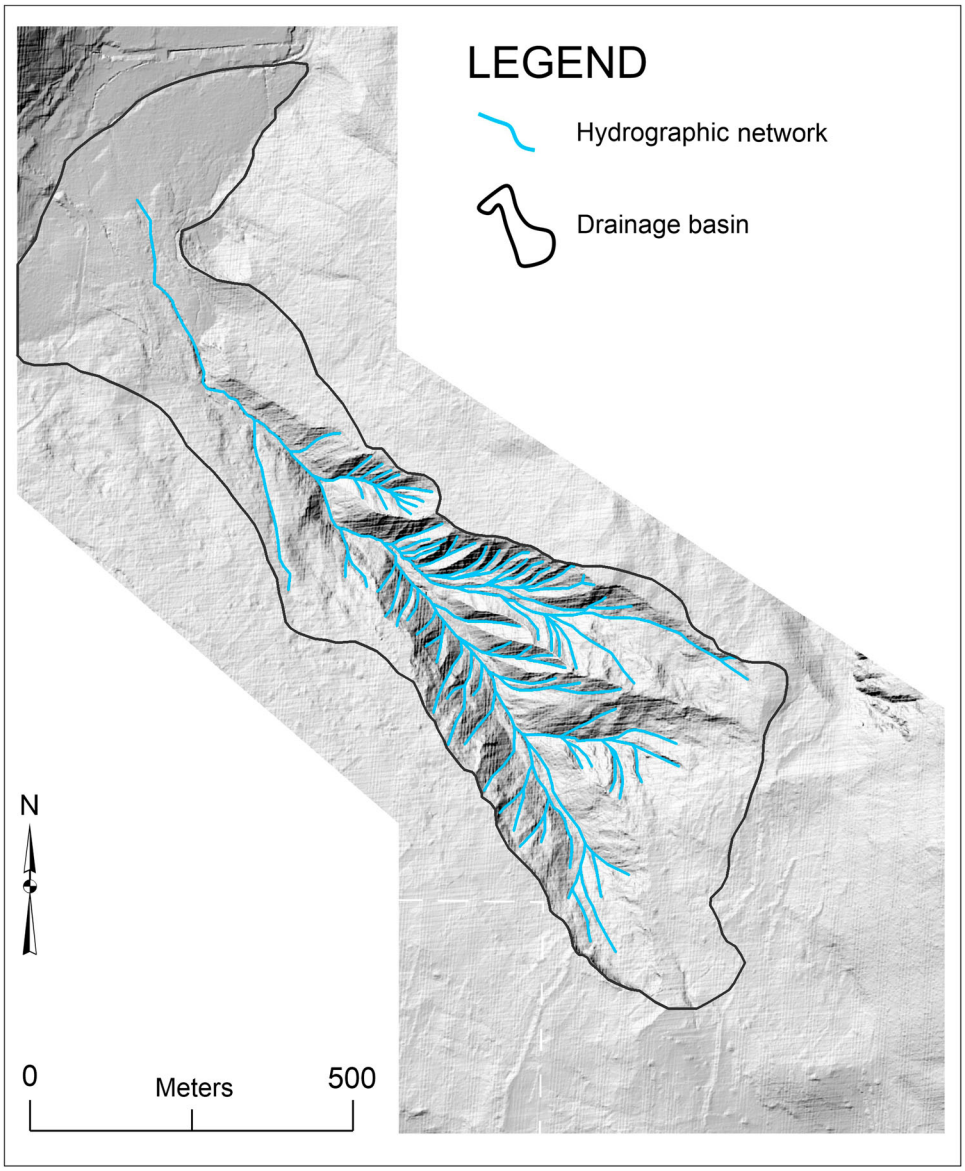

Figure 3. Study area drainage basin and hydrographic network map.

4.2.3.3. Landslide deposits (4). They are compounded of clayey-silty material, locally with gypsum presence, and involve the bedrock unit of the terrigenous slope (Figure 4(c)). This unit refers to the Holocene (Miccadei et al., 2014).

4.2.3.4. Colluvial deposits (3). This unit consists of clays, silt, and sands with decimetric calcareous clasts (Figure 4d). It outcrops at the base of the badlands area, above debris-mud flow deposits (1), with an erosive limit and it refers to Holocene (Miccadei et al., 2014).

4.2.3.5. Fluvial deposits (2). They are composed of heterometric pebbles with sandy and silty levels (Figure 4 (e)). They are present in correspondence of the Sagittario River and are related to Holocene (Miccadei et al., 2014).

4.2.3.6. Debris-mud flow deposits (1). This unit consists of reworked clays, silts, and heterometric blocks of crystalline gypsum with a chaotic setting. They are present in the main gullies (Figure 4(f)) and in correspondence of the alluvial fan, at the base of *calanchi*. They are dated to Holocene (Miccadei et al., 2014).

4.3. Geomorphology

The main geomorphological features were classified and distinguished according to the morphogenetic environment. Predominant morphologies are represented by structural, slope-gravity, and fluvial landforms (Figure 5).

4.3.1. Structural landforms

The predominant structural landform, showing an NW–SE direction, is represented by a fault line scarp in the lower right side of the main map (Figure 5(a)) between the dolomitic limestones (8) and the clays (7).

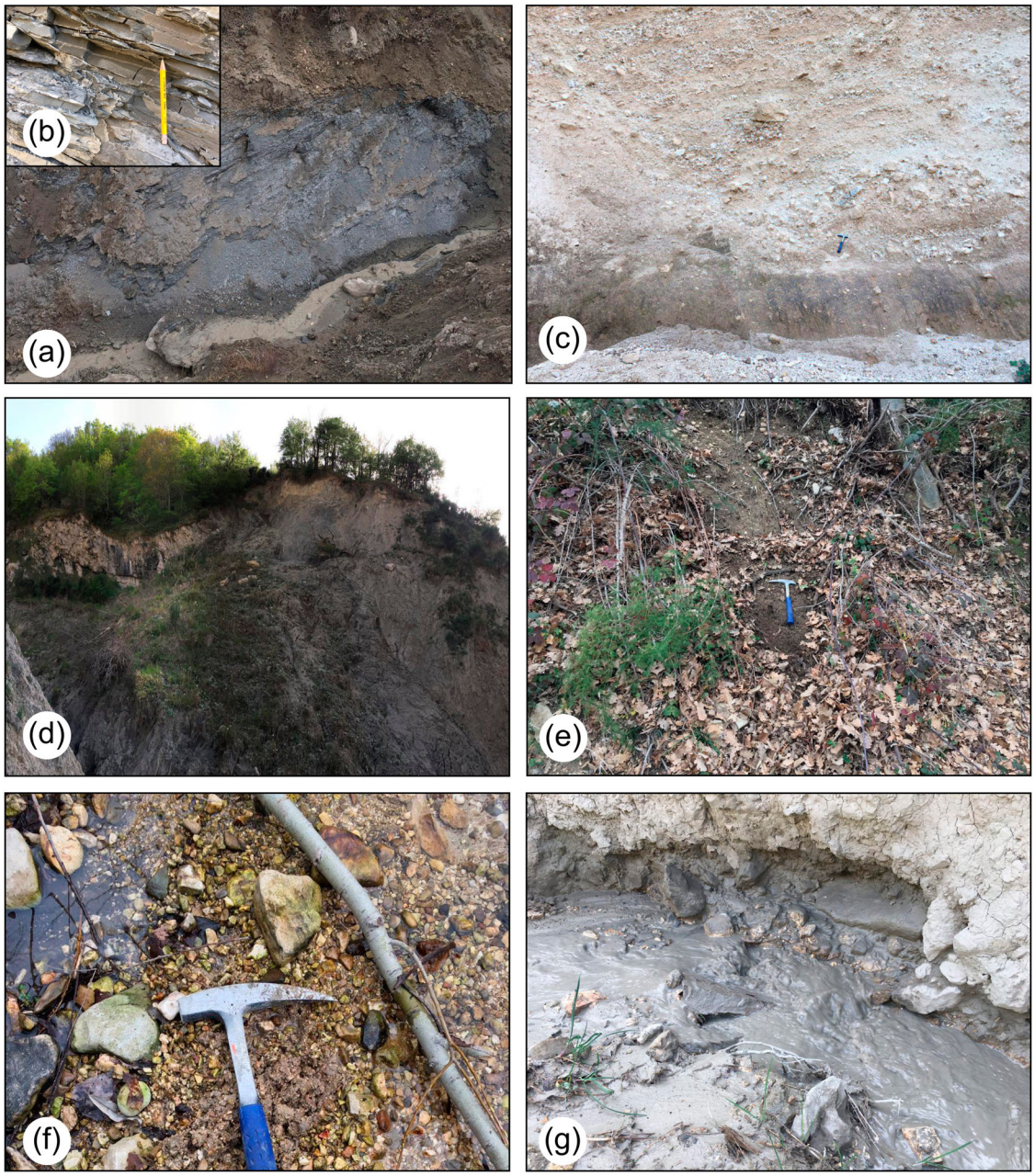

Figure 4. Post-orogenic continental deposits and syn-orogenic marine deposits of the study area (numbers are referred to the main legend). (a) well-stratified fetid silty clay (7) (a zoomed view is in the upper right corner); (b) cemented-to-loose stratified slope deposits (6); (c) landslide deposits with chaotic material and toppled trees (5); (d) colluvial deposits made of loose sands and silts (3); (e) fluvial deposits with sand and silt levels (2); (f) debris-mud flow deposits with active transport of mud and reworked material (1).

4.3.2. Slope-gravity landforms

These mapped elements include different types of landslides with associated scarps. Landslides (Figure 5(c)) are located especially in the SW sector of the badland area and they are principally related to both active earth flows and complex landslides. The related landslide scarps are all main gully-oriented (SW–NE, SE–NW, and E–W).

4.3.3. Fluvial landforms

The mapped fluvial landforms can be referred to active gullies, sharp and rounded crests, V-shaped and U-shaped valleys, flooding channels, and alluvial fan. Gullies (Figure 5(b)) are the most important features of the study area. There is a principal gully which describes a deep incision (SE–NW oriented) with a flat bottom approaching the intermediate sector and other gullies starting at the outlets of the furrows. Sharp and rounded crests are parallel to the valleys; V-shaped and U-shaped valleys evolution is strictly linked to water availability (Figure 5(d)). Flooding channels and alluvial fan are located at the base of the badlands and their presence is related to the volume of material transported by debris-mud flows and water, so they are extremely variable. Alluvial fan (Figure 5(f)) is located at the bottom of the badlands. Rill erosion is

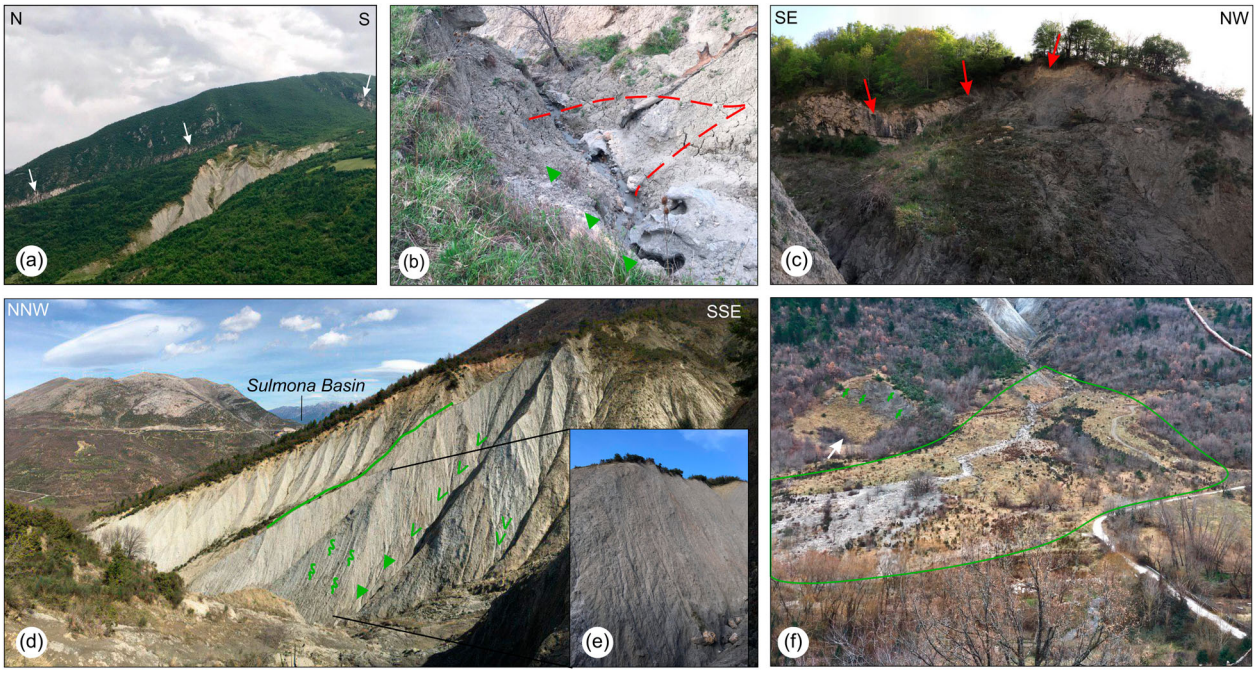

Figure 5. Geomorphological features of the study area. (a) fault line scarp (white arrows); (b) active gully erosion with visible water flow and weathered substratum; (c) landslide affecting the left slope of the badlands (the red arrows indicate the scarp); (d) panoramic view of the study area in which the main geomorphological features are visible: the badlands boundary, V-shaped valleys, sharp crests and gullies (not all the features were marked in this photo); (e) zoomed view of the rill erosion. (f) panoramic view of the flooding fan (green polygon); the white arrows indicate the inactive quarry where active slope wash is present.

diffused over almost all slopes (Figure 5(e)). Sheet erosion affects the right slope of the main badlands, where the clayey substrate is washed out and a degradational scarp is present (Figure 5(f)).

4.3.4. Anthropogenic landforms

This landform is linked to a little scarp located on the right side of the badlands. It is related to an old and disused quarry where clay was extracted to produce post-medieval pottery (Verrocchio, 2003).

4.3.5. Vegetation cover

Vegetation cover consists of wood and sparse vegetation and colluvial material with a maximum thickness of 3 m.

4.4. Multi-temporal analysis

The multi-temporal analysis of the badlands area was outlined by means of air-photos stereoscopy (according to Amadesi, 1993), and orthophotos interpretation in GIS environment in order to provide quantitative data about the geomorphological evolution badlands area from 1954 to 2017 (see Table 3 for further information about air-photos). We considered the incised area and alluvial fan area separately.

The analysis of the badlands area on 1954 air-photos (198,760 m^2, Figure 6(a)) highlights a stretched morphology, with a slightly extended alluvial fan. The active sector is on the left side, while on the right one, the vegetation cover is present. The hydrographic pattern is mainly dendritic, with several 90° confluences highlighted by minor and ephemeral stream channels. The 1997 air-photos analysis (Figure 6(b)) shows an increase of the area to ~237,000 m^2. The active sector is on the right side and at the initial sector of the alluvial fan; this feature is now developed in the NE direction. On the SE sector, there is an evident ESE-SE slope retirement due to the slope-gravity process, as confirmed by geomorphological field investigations. In the 2007 orthophoto (Figure 6(c)) the badlands area reaches ~ 245,000 m^2, showing a dendritic hydrographic pattern. The active sector is at the center of the alluvial fan. The Google Earth 2017 image analysis (Figure 6(d)) shows a further increase of the badlands and the alluvial fan areas. The active sector is located in small areas at the base of the badlands,

Table 3. Parameters regarding to the aerial photos and orthophotos used in this work, (modified Del Soldato et al., 2018).

Organization	Acquisition year	Approximate scale	Type	Flying height (m)
I.G.M.	1954	1:33,000	Aerial photos	~6000
AIMA	1997	1:10,000	Orthophotos	–
Abruzzo Region	2007	1:5000	Orthophotos	~2000
Google Earth	2017	1:1000	Satellite image	–

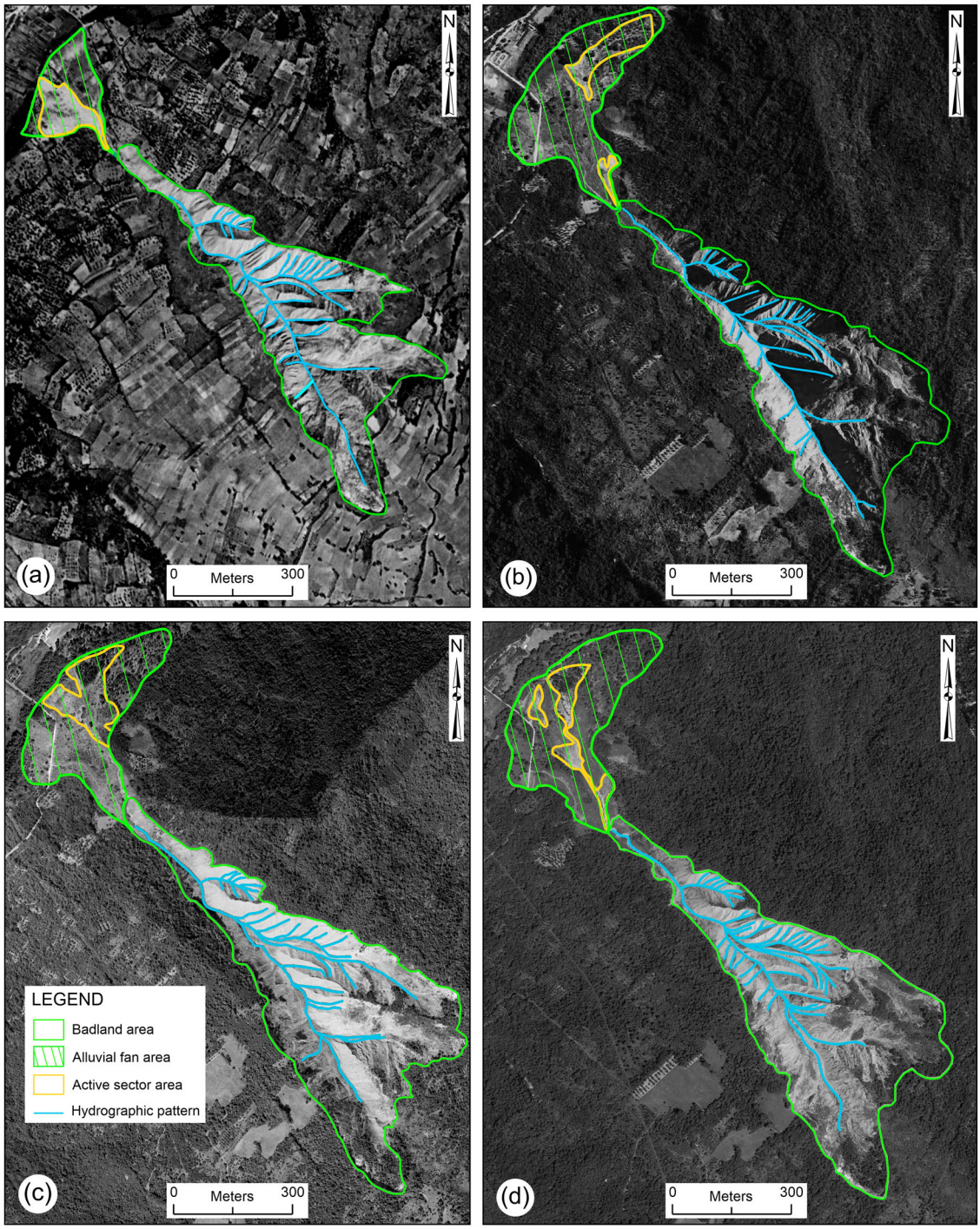

Figure 6. Multi-temporal evolution analysis of the 'il Caccavone' badlands area (we changed RGB to B/W to improve the readbility). (a) IGMI, 1954 aerial photo; (b) Abruzzo Region (1997) orthophoto; (c) Abruzzo Region (2007) orthophoto; (d) Google Earth (2017) satellite photo. All photos have been changed to black and white in order to improve the readbility (see also the main map, Multi-temporal analysis of the badlands area section). The legend refers to all the four images.

moving towards the Sagittario River. The hydrographic pattern type is still dendritic and more ramifications due to minor and ephemeral stream channels are evident.

5. Conclusions

The detailed geomorphological analysis of the Anversa degli Abruzzi badlands area led to the recognition of geomorphological processes that control the morphometry of this badlands system. It was performed following a multidisciplinary approach involving morphometric, geomorphological and multi-temporal analysis.

The orographic setting is described by high values of slope (>50°) in the southern exposures located in correspondence of heavy rill erosion areas. The northern slopes are characterized by landslides and vegetative covers, probably due to a higher water amount.

The hydrographic setting was analyzed through the calculation of several morphometric parameters. Particularly, the Melton ratio gives a value of 0.719

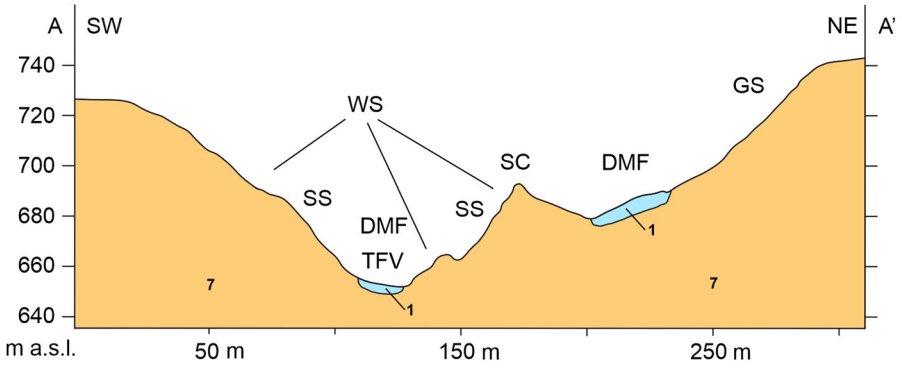

Figure 7. Schematic geomorphological profile (for the trace ubication, A-A', see on the Figure 1(b)) to show type 'B' badlands features. From left to right: (SS) steep slopes; (DMF) debris-mud flow; (TFV) trough-floored valley; (WS) weathered slopes; (SC) sharp crest; (GS) gentle slope. The scale is given by horizontal and vertical numbers. Vertical numbers are referred to the mean sea level. The numbers will refer to the lithological legend of the main map: (1) Debris-mud flow deposits; (7) Clays.

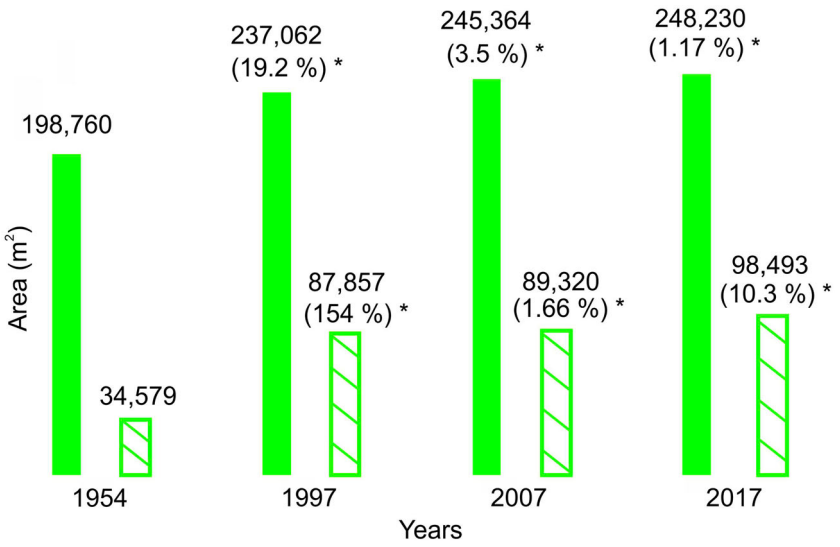

Figure 8. Histogram showing evolution trend. Blue boxes stand for badland area; cobalt blue boxes stand for alluvial fan area; ()* percentage is referred to the increase of values with respect to the previous measurement.

(Melton constant is 0.694), and D^2 is less than 0.001 (Di Stefano & Ferro, 2019). Also, the L/P ratio is bigger than 40 m/° (Buccolini & Coco, 2010). These values indicate a dendritic hydrographic pattern, thus confirming the field data.

The detailed geomorphological field survey highlighted the relationships between landforms and deposits, as graphically shown in the schematic geomorphological profile (Figure 6). In detail, debris-mud flow deposits are linked to gully erosion, but they are not distributed all over the incisions; landslides are related to complex, earth flows and debris-mud flows kinematics. Gullies and V-shaped valleys are the main fluvial landforms which affect the badlands area. The *calanchi* landform is classifiable as type 'B' (Moretti & Rodolfi, 2000), with steep slopes, sharp and rounded crests, superficially weathered substratum and superficial slides, as you can see in schematic section below (Figure 7; see also the Figure 1 for the section trace).

The multi-temporal photogeological analysis led to reconstruct the geomorphological evolution. The 1954–2017 (Figure 8) interval shows an increase of the eroded area from 198,760 to 248,230 m^2 (increase of 24.8%); erosive processes include mainly slope-gravity and rill erosion. The biggest landslides affect the highest topographic sectors of the badlands, highlighted by an active retirement towards SE direction. Between 1954 and 1997, the right slope was involved in landslide processes. Alluvial fan is significantly increased between 1954 and 1997 (~154%); the evolution of this element is strictly related to the water and sediment amount coming from valleys and gullies; 90° confluences seem to be reduced and the hydrographic pattern became perfectly dendritic. The right top of the badlands is characterized by the ancient slope deposits (6) involved in the erosion, so it is possible to affirm that there is a reduction of this unit volume. Alluvial fan sediments are probably eroded by the Sagittario River, and in combination with the

water runoff amount, percentage values between the fan and the badlands areas maybe not directly proportional. Finally, three main factors were linked to the geomorphological evolution: water runoff and landslide processes, and aspect of the slopes.

This study could represent a scientific basis for the understanding of the Anversa degli Abruzzi badlands area, giving a key tool to better highlight the main phases of the evolution in terms of geomorphological processes of this typical Italian landscape.

Software

The map presented was produced in the Geographic Information System ArcGis® 10.6.1 (ESRI); the final editing of the map and photos was made with CorelDRAW 2019 v21.

Acknowledgements

The authors wish to thank the Struttura Speciale di Supporto Sistema Informativo Regionale (http://www.regione.abruzzo.it/xcartografia), the Open Geodata service (http://opendata.regione.abruzzo.it/) and the Google Earth software (https://www.google.it/intl/it/earth/) for providing aerial photos used for the geomorphological investigations. We also thank the Ministry of Environment (National Geoportal, http://www.pcn.minambiente.it/) for providing Digital Elevation Models derived from 1 m LiDAR data.

The authors are also grateful to the reviewers Professor V. Ferro, Dr M. Del Soldato, and Dr von Wyss, whose suggestions greatly improved the manuscript and the map.

Disclosure statement

No potential conflict of interest was reported by the author (s).

Funding

The work was supported by Università degli Studi 'G. d'Annunzio' Chieti Pescara funds (E. Miccadei University fund).

ORCID

Jacopo D'Intino http://orcid.org/0000-0003-1371-7302
Marcello Buccolini http://orcid.org/0000-0002-3880-1298
Gianluca Esposito http://orcid.org/0000-0002-6077-9920
Enrico Miccadei http://orcid.org/0000-0003-2114-2940

References

Abruzzo Region. (1997). 1:10,000 scale orthophotos black and white images. http://geocatalogo.regione.abruzzo.it/erdas-iws/ogc/wms/?

Abruzzo Region. (2007). 1:5,000 scale orthophotos color images. Retrieved from opendata.regione.abruzzo.it/content/ortofoto-regione-abruzzo-2007.

Alexander, D. E. (1980). The calanchi accelerated erosion in Italy. *Geography Compass*, *65*, 95–100.

Amadesi, E. (1993). *Manuale di fotointerpretazione con elementi di fotogrammetria*. Pitagora.

Ascione, A., Cinque, A., Miccadei, E., Villani, F., & Berti, C. (2008). The plio-quaternary uplift of the Apennine chain: New data from the analysis of topography and river valleys in Central Italy. *Geomorphology*, *102*(1), 105–118. https://doi.org/10.1016/j.geomorph.2007.07.022

Beneo, E. (1938). Insegnamenti di una galleria a proposito della tettonica nella Valle del Sagittario (Appennino abruzzese). *Bollettino Regio Ufficio Geologico Italiano*, *63* (6), 1–10.

Buccolini, M., & Coco, L. (2010). The role of the hillside in determining the morphometric characteristics of 'calanchi': The example of Adriatic central Italy. *Geomorphology*, *123*(3–4), 200–210. https://doi.org/10.1016/j.geomorph.2010.06.003

Buccolini, M., & Coco, L. (2013). MSI (morphometric slope index) for analyzing activation and evolution of calanchi in Italy. *Geomorphology*, *191,* 142–149. https://doi.org/10.1016/j.geomorph.2013.02.025

Buccolini, M., Coco, L., Cappadonia, C., & Rotigliano, E. (2012). Relationships between a new slope morphometric index and calanchi erosion in northern Sicily, Italy. *Geomorphology*, *149–150,* 41–48. https://doi.org/10.1016/j.geomorph.2012.01.012

Calista, M., Miccadei, E., Pasculli, A., Piacentini, T., Sciarra, M., & Sciarra, N. (2016). Geomorphological feratures of the Montebello sul Sangro large landslide (Abruzzo, Central Italy). *Journal of Maps*, *12*(5), 882–891. https://doi.org/10.1080/17445647.2015.1095134

Capelli, G., Miccadei, E., & Raffi, R. (1997). Fluvial dynamics in the Castel di Sangro plain: Morphological changes and human impact from 1875 to 1992. *Catena*, *30*(4), 295–309. https://doi.org/10.1016/S0341-8162(97)00008-8

Caraballo-Arias, N. A., Conoscenti, C., Di Stefano, C., & Ferro, V. (2015). A new empirical model for estimating calanchi erosion in Sicily, Italy. *Geomorphology*, *231*, 292–300. https://doi.org/10.1016/j.geomorph.2014.12.017

Caraballo-Arias, N. A., & Ferro, V. (2017). Are calanco landforms similar to river basins? *Science of Total Environment*, *603-604*, 244–255. https://doi.org/10.1016/j.scitotenv.2017.06.009

Carabella, C., Miccadei, E., Paglia, G., & Sciarra, N. (2019). Post-Wildfire Landslide Hazard Assessment: The Case of The 2017 Montagna Del Morrone Fire (Central Apennines, Italy). *Geosciences*, *9*(4), 175. Switzerland. https://doi.org/10.3390/geosciences9040175

Carminati, E., & Doglioni, C. (2012). Alps vs Apennines: The paradigm of a tectonically asymmetric Earth. *Earth-Science Reviews*, *112*(1–2), 67–96. https://doi.org/10.1016/j.earscirev.2012.02.004

Cassetti, M. (1900). Rilevamenti geologici eseguiti l'anno 1899 nell'alta Valle del Sangro e in quella del Sagittario, del Gizio e del Melfa. *Bollettino del Comitato Geologico Italiano*, *31*, 255–272.

Castiglioni, B. (1933). Osservazioni sui calanchi appenninici. *Bollettino Della Società Geologica Italiana*, *52*, 357–360.

Ciccacci, S., D'Alessandro, L., Dramis, F., & Miccadei, E. (1999). Geomorphologic evolution and neotectonics of the Sulmona intramontane Basin (Abruzzi Appennine, Central Italy). *Z. Geomorph. N.F., Supp*, *118*, 27–40.

Ciccacci, S., Galiano, M., Roma, M. A., & Salvatore, M. C. (2008). Morphological analysis and erosion rate evaluation in badlands of Radicofani area (Southern Tuscany – Italy). *Catena*, *74*(2), 87–97. https://doi.org/10.1016/j.catena.2008.03.012

Coltorti, M., Dramis, F., Gentili, B., & Pambianchi, G. (1979). Stratified slope deposits in the Umbria-Marche Apennines. *Proc. 15th Meeting "Geomorphological Survey & Mapping"*, Modena.

Corrado, S., Miccadei, E., Parotto, M., & Salvini, F. (1996). Evoluzione tettonica del settore di Montagna Grande (Appennino centrale): il contributo di nuovi dati geometrici, cinematici e paleogeotermici. *Bollettino Della Società Geologica Italiana*, *115*, 325–338. Roma.

Del Soldato, M., Riquelme, A., Tomás, R., De Vita, P., & Moretti, S. (2018). Application of structure from motion photogrammetry to multi-temporal geomorphological analyses: Case studies from Italy and Spain. *Geogr. Fis. Dinam. Quat*, *41*, 51–66. https://doi.org/10.4461/GFDQ.2018.41.4

Demangeot, J. (1965). Neotectonique du Gran Sasso (Appennin central). *Review of Physical Geography and Dynamic Geology*, *7*, 223–234.

Di Lena, B., Antenucci, F., & Mariani, L. (2012). Space and time evolution of the Abruzzo precipitation. *Italian Journal of Agrometeorology*, *1*, 5–20.

Di Stefano, C., & Ferro, V. (2019). Assessing sediment connectivity in dendritic and parallel calanchi systems. *Catena*, *172*, 647–654. https://doi.org/10.1016/j.catena.2018.09.023

D'Orefice, M., & Graciotti, R. (2014). Rilevamento geomorfologico e cartografia. Realizzazione – Lettura – Interpretazione. *Dario Flaccovio Editore*.

Farabollini, P., Gentili, B., & Pambianchi, G. (1992). Contributo allo studio dei calanchi: Due aree campione nelle Marche. *Studi Geologici Camerti*, *12*, 105–115. Camerino.

Ghisetti, F., & Vezzani, L. (1993). Transpressioni destre nelle zone esterne dell'Appennino centrale. *Geologica Romana*, *29*, 73–95. Roma.

Google. (2017). Google Earth satellite color images. Retrieved from Google Earth software.

Horton, R. E. (1945). Erosional development of streams and their drainage basins; hydrophysical approach to quantitative morphology. *Geological Society American Bulletin*, *56*(3), 275–370. https://doi.org/10.1130/0016-7606(1945)56[275:EDOSAT]2.0.CO;2

IGMI. (1954). 1:33.000 scale aerial photos of Flight GAI. Istituto Geografico Militare Italiano.

ISIDe Working Group. (2016). Italian seismological instrumental and parametric database (ISIDe). *Instituto Nazionale di Geofisica e Vulcanologia (INGV)*. https://doi.org/10.13127/ISIDe

ISPRA. (2014). Carta Geologica d'Italia alla scala 1:50.000, Foglio 378 'Scanno'. Servizio Geologico d'Italia. ISPRA. Retrieved from http://www.isprambiente.gov.it/Media/carg/378_SCANNO/Foglio.html

Magny, M., Miramont, C., & Sivan, O. (2002). Assessment of the impact of climate and anthropogenic factors on Holocene Mediterranean vegetation in Europe on the basis of palaeohydrological records. *Palaeo*, *186*(1–2), 47–59. https://doi.org/10.1016/S0031-0182(02)00442-X

Mattei, M., & Miccadei, E. (2001). Strike-slip tectonics between the Marsica range and the Molisan basin in the Sangro valley (Abruzzi, Central Italy). *Bollettino Della Società Geologica Italiana*, *110*, 737–745. Roma.

Melton, M. A. (1957). An analysis of relations among elements climate, surface properties and geomorphology. Project nr. 389-042, Tech. Rep., 11, Columbia University, Department of Geology, ONR.

Miccadei, E. (1993). Geologia dell'area Alto Sagittario – Alto Sangro (Abruzzo, Appennino centrale). *Geologica Romana*, *29*, 463–481. Roma.

Miccadei, E., Barberi, R., & Cavinato, G. P. (1998). La Geologica quaternaria della Conca di Sulmona (Abruzzo, Italia centrale). *Geologica Romana*, *34*, 59–86.

Miccadei, E., Berti, C., Calista, M., Esposito, G., Mancinelli, V., & Piacentini, T. (2019). Morphotectonics of the Tasso stream – Sagittario River valley (Central Apennines, Italy). *Journal of Maps*, *15*(2), 257–268. https://doi.org/10.1080/17445647.2019.1589588

Miccadei, E., Carabella, C., Paglia, G., & Piacentini, T. (2018). Paleo-Drainage network, morphotectonics, and fluvial terraces: Clues from the Verde stream in the middle Sangro River (Central Italy). *Geosciences*, *8*(9), 337. https://doi.org/10.3390/geosciences8090337

Miccadei, E., D'Alessandro, L., Parotto, M., Piacentini, T., & Praturlon, A. (2014). Note illustrative alla Carta Geologica d'Italia (scala 1:50.000), Foglio 378 'Scanno'. *Servizio Geologico d'Italia, ISPRA*, Roma.

Miccadei, E., Piacentini, T., & Buccolini, M. (2017). Long-term geomorphological evolution in the Abruzzo area, Central Italy: Twenty years of research. *Geologica Carpathica*, *68*(1), 19–28. https://doi.org/10.1515/geoca-2017-0002

Miccadei, E., Piacentini, T., Gerbasi, F., & Daverio, F. (2012). Morphotectonic map of the Osento River basin (Abruzzo, Italy), scale 1:30,000. *Journal of Maps*, *8*(1), 62–73. https://doi.org/10.1080/17445647.2012.668764

Miller, V. C. (1953). *A quantitative geomorphic study of drainage basin characteristics in the Clinic Mountain area, Virginia and Tennesse* (Project NR 389-042, Tech. Recpt., 3). Columbia Univ. Dept. of Geology. O.N.R. Geographic Branch.

Moretti, S., & Rodolfi, G. (2000). A typical 'calanchi' landscape on the eastern Apennine margin (Atri, Central Italy): geomorphological features and evolution. *Catena*, *40*(2), 217–228. https://doi.org/10.1016/S0341-8162(99)00086-7

Neugirg, F., Stark, M., Kaiser, A., Vlacilova, M., Della Seta, M., Vergari, F., Schmidt, J., Becht, M., & Haas, F. (2016). Erosion processes in calanchi in the Upper Orcia Valley, Southern Tuscany, Italy based on multitemporal high-resolution terrestrial LiDAR and UAV surveys. *Geomorphology*, *269*, 8–22. https://doi.org/10.1016/j.geomorph.2016.06.027

Nisio, S., Prestininzi, A., & Scarascia Mugnozza, G. (1996). I calanchi del settore settentrionale della fascia periadriatica abruzzese: Quadro morfotettonico e loro caratterizzazione. *Studi Geologici Camerti*, *14*, 29–45.

Piacentini, T., & Miccadei, E. (2014). The role of drainage systems and intermontane basins in the quaternary landscape of the Central Apennines chain (Italy). *Rend. Fis. Acc. Lincei*, *25*(139), https://doi.org/10.1007/s12210-014-0312-2

Piacentini, T., Urbano, T., Sciarra, M., Schipani, I., & Miccadei, E. (2015). Geomorphology of the floodplain at the confluence of the Aventini and Sangro rivers (Abruzzo, Central Italy). *Journal of Maps, 12*(3), 443–461. https://doi.org/10.1080/17445647.2015.1036139

Rodolfi, G., & Frascati, F. (1979). Cartografia di base per la programmazione degli interventi in aree marginali (area rappresentativa della Val d'Era). *Annali Istituto per lo Studio e la Difesa del Suolo*, *10*.

Rovida, A., Locati, M., Camassi, R., Lolli, B., & Gasperini, P. (2019). Catalogo Parametrico dei Terremoti Italiani (CPTI15), versione 2.0. *Instituto Nazionale di Geofisica e*

Vulcanologia (INGV), https://doi.org/10.13127/CPTI/CPTI15.2

Salvador, A. (1994). International stratigraphic guide. A guide to stratigraphic classification, terminology, and procedure. The International Union of Geological Sciences and the Geological Society of America (eds.) (p. 214).

SGN. (1994). Guida al rilevamento della Carta Geomorfologica d'Italia, 1:50.000. *Quaderni Serie III del Servizio Geologico Nazionale*, *4*, 1–151. Roma.

Strahler, A. N. (1957). Quantitative analysis of watershed geomorphology. *Transaction, American Geophysical Union*, *38*(6), 913–920. https://doi.org/10.1029/TR038i006p00913

Twidale, C. R. (2004). River patterns and their meaning. *Earth-Science Reviews*, *67*(3-4), 159–218. https://doi.org/10.1016/j.earscirev.2004.03.001

Vergari, F., Troiani, F., Faulkner, H., Del Monte, M., Della Seta, M., Ciccacci, S., & Fredi, P. (2019). The use of the slope–area function to analyze process domains in complex badland landscapes. *Earth Surface Processes and Landforms*, *44*(1), 273–286. https://doi.org/10.1002/esp.4496

Verrocchio, V. (2003). La ceramica postmedievale di Anversa degli Abruzzi (AQ). Fonti archivistiche ed archeologiche. *Archeologia Postmedievale*, *7*, 93–121.

Vezzani, L., Festa, A., & Ghisetti, F. (2010). Geology and tectonic of the Central-Southern Apennines, Italy. *Geological Society of America*, *469*, https://doi.org/10.1130/2010.2469

Vittorini, F. (1971). La degradazione in un campo sperimentale nelle argille plioceniche della Val d'Era (Toscana) e i suoi riflessi morfogenetici. *Rivista Geografica Italiana*, *78*, 142–169.